

Experimental Identification of Nonideal Two-qubit Quantum-state Filter by Quantum Process Tomography

Yoshihiro Nambu and Kazuo Nakamura
*Fundamental and Environmental Research Laboratories,
 NEC, 34 Miyukigaoka, Tsukuba, Ibaraki 305-8501, Japan*

We investigated nonideal two-qubit quantum-state filter subject to various degree of decoherence by quantum process tomography and identified its function. We present a simple decoherence model that explains the experimental results, and point out that the common belief that a beamsplitter with post-selecting coincidence signals works as a singlet-state filter is erroneous. In the ideal case it should be a triplet-state filter.

PACS numbers: 03.65.Wj, 42.50.Dv

Characterization of quantum devices is important in the development of quantum computing. In particular, the characterization of single- and two-qubit devices is important because a single-qubit rotation gate and a two-qubit controlled-NOT (C-NOT) gate are two building blocks of the quantum computer[1]. Since actual devices may couple to their environment, resulting in decoherence and nonunitary state evolution, identifying and understanding the function of the actual devices is important for developing the devices. Nonideal quantum devices can be characterized by quantum process tomography (QPT)[2, 3, 4]. QPT has been used to characterize single-qubit transmission channels for photons [5, 6], single-qubit rotation gates for photons [7], gates for ensembles of two-qubit systems in NMR[8], a two-qubit quantum-state filter for photons[9], and a two-qubit C-NOT gate for photons[10].

This letter reports the QPT of a quantum-state filter: the beamsplitter (BS) in a Hong-Ou-Mandel (HOM) interferometer[11, 12], as a demonstration of experimental identification of two-qubit device. The ideal filter has already been investigated[9] and the function were found to be different from what had been thought previously[12, 13], but the reason for this difference was not fully understood. We have studied the reason by investigating the function of the nonideal filter with decoherence. We could identify major and noise contributions to the operator-sum representation of quantum operation for this nonideal filter.[1, 2, 14] We present a model that explains our experimental results and show the above reason as well as the error in a common belief about the function of the BS in a HOM interferometer.

Let us start by introducing the process matrix[10], which offers us the most general description of the quantum device allowed in quantum mechanics, and showing how to obtain it experimentally. Consider a two-qubit device whose function is to map a two-qubit input density operator ρ_{in} to a two-qubit output density operator $\rho_{out} = \mathcal{E}(\rho_{in})$, where \mathcal{E} is a completely positive linear map[14]. The map \mathcal{E} is considered a superoperator acting on positive operators[15]. If we introduce the standard operator basis $\{X_{\langle ij \rangle} = |i\rangle\langle j|\} (i, j = 0, 1)$ [16], where

$\langle ij \rangle := 2i + j$, \mathcal{E} can be expanded as

$$\mathcal{E}(\rho) = \sum_{\substack{i,j,k,l, \\ m,n,o,p=0}}^1 (\chi^S)_{[\langle ij \rangle \langle kl \rangle][\langle mn \rangle \langle op \rangle]} X_{\langle ij \rangle} \otimes X_{\langle kl \rangle} \rho X_{\langle mn \rangle}^\dagger \otimes X_{\langle op \rangle}^\dagger, \quad (1)$$

where $[kl] := 4k+l$ ($k, l = 0, \dots, 3$)[15]. A 16×16 positive Hermitian matrix χ^S fully characterizes the function of quantum device and is called the process matrix in the standard operator basis[10].

We can transform χ^S into the process matrix in any two-qubit operator basis $\{A_\alpha\}$ ($\alpha = 0, \dots, 15$) that spans the two-qubit operator space. Note that A_α may be defined either locally or nonlocally. For example, the Kronecker products of the Pauli operator basis $E_i \otimes E_j$ ($i, j = 0, \dots, 3$), where $\{E_i\} = \{\sigma_0/\sqrt{2}, \sigma_1/\sqrt{2}, \sigma_2/\sqrt{2}, \sigma_3/\sqrt{2}\}$ and σ_0 denotes an identity operator, is a local operator basis, whereas the outer product $|\Phi_i\rangle\langle\Phi_j|$ ($i, j = 0, \dots, 3$), where $|\Phi_i\rangle$ are Bell states, is a nonlocal one. The basis $\{A_\alpha\}$ is, in general, unitarily related to the standard basis $\{X_\alpha\}$. That is, $A_\alpha = \sum_{k,l=0}^3 (U)_{[kl]\alpha} X_k \otimes X_l$, where U is a 16×16 unitary matrix. Then \mathcal{E} can be expanded using A_α as follows:

$$\mathcal{E}(\rho) = \sum_{\alpha,\beta=0}^{15} (\chi^A)_{\alpha\beta} A_\alpha \rho A_\beta^\dagger, \quad (2)$$

where $\chi^A = U^\dagger \chi^S U$. Therefore, χ^A is given by the unitary transform of χ^S .

To obtain χ^S , it is sufficient to determine the associated four-qubit state[17]. Let us consider a four-qubit system composed of the two two-qubit systems 1-2 and 3-4 and introduce the unnormalized maximally entangled state $|I\rangle\rangle = \sum_{i=0}^1 |i, i\rangle$ [4, 16]. Let us introduce the unnormalized four-qubit density operator $\mathcal{D}_\mathcal{E}$ associated with \mathcal{E} by $\mathcal{D}_\mathcal{E} = \mathcal{E}^{(13)} \otimes \mathcal{I}^{(24)}(|I\rangle\rangle_{12} \langle\langle I| \otimes |I\rangle\rangle_{34} \langle\langle I|)$, where \mathcal{I} is an identity map and the superscript and subscript respectively denote the space on which each map acts and the space to which the operator belongs[17]. By using the identity $(X_{\langle ij \rangle} \otimes I)|I\rangle\rangle \equiv |i, j\rangle$ and Eq. 1, we can

rewrite $\mathcal{D}_\mathcal{E}$ as

$$\mathcal{D}_\mathcal{E} = \sum_{\substack{i,j,k,l, \\ m,n,o,p=0}}^1 (\chi^S)_{[(ij)\langle kl\rangle][\langle mn\rangle\langle op\rangle]} |i, j, k, l\rangle \langle m, n, o, p|. \quad (3)$$

Equations 1 and 3 indicate that the process matrix in the standard operator basis agrees exactly with the density matrix of the associated state in the standard basis. Evaluation of the process matrix is thus reduced to evaluation of the associated state $\mathcal{D}_\mathcal{E}$.

To obtain $\mathcal{D}_\mathcal{E}$, it is sufficient to evaluate all the maps $\mathcal{E}(X_{\langle ij\rangle} \otimes X_{\langle kl\rangle})$ for all the elements of the standard operator basis on two-qubit space $\{X_{\langle ij\rangle} \otimes X_{\langle kl\rangle}\}$, since we can obtain the permutation equivalent of $\mathcal{D}_\mathcal{E}$ —that is, $\tilde{\mathcal{D}}_\mathcal{E} = P_{23}P_{12}P_{34}\mathcal{D}_\mathcal{E}P_{34}P_{12}P_{23} = \mathcal{I}^{(12)} \otimes \mathcal{E}^{(34)}(|I\rangle)_{13}\langle\langle I| \otimes |I\rangle)_{24}\langle\langle I|$ —by using the following identity:

$$\tilde{\mathcal{D}}_\mathcal{E} \equiv \sum_{i,j,k,l=0}^1 X_{\langle ij\rangle} \otimes X_{\langle kl\rangle} \otimes \mathcal{E}(X_{\langle ij\rangle} \otimes X_{\langle kl\rangle}), \quad (4)$$

where P_{ij} is a permutation operator between the systems i and j . To evaluate these maps, we need only to use state tomography[18] to evaluate the 16 two-qubit output states $\{\mathcal{E}(\rho_{12})\}$ associated with 16 separable input states $\{\rho_{12}\} = \{\rho_1 \otimes \rho_2\}$; $\rho_i \in \{|0\rangle\langle 0|, |1\rangle\langle 1|, |+\rangle\langle +|, |\odot\rangle\langle \odot|\}$, where $|+\rangle = 1/\sqrt{2}(|0\rangle + |1\rangle)$ and $|\odot\rangle = 1/\sqrt{2}(|0\rangle + i|1\rangle)$ [2, 3, 4]. We therefore can obtain the process matrix directly from the experimental data without using a matrix inversion procedure[1, 2].

We used the above procedure to obtain the process matrices for nonideal two-qubit quantum-state filters. The experimental setup is shown in Fig. 1. A 0.3-mm-thick type-I crystal (BBO) was pumped by frequency-tripled pulses generated by 100-fs pulses from the mode-locked Ti:sapphire laser (repetition rate ≈ 82 MHz). Pairs of horizontally polarized photons at 532 nm were generated and those traveling in two directions 9° from the pump beam were selected by 5-mm irises (1 m from the crystal) and identical 3-nm-width filters (IF) placed before the detectors. They were injected into a HOM interferometer[9, 11, 12] having a cube BS with a wide-band multilayer dielectric coating on an interface. The horizontally (H) and vertically (V) polarized states (respectively $|0\rangle$ and $|1\rangle$) and the other two states required for the QPT were prepared by half- and quarter-wave plates (HWP and QWP) placed immediately before the BS. Down-converted photons were incident on the BS at 45° . After the BS, polarization analyzers consisting of a QWP and a HWP followed by a Glan-Thompson prism (POL) and a single-photon counting module (PMT) performed projective measurements onto the 16 product states $\{\rho_{12}\}$. Only signals coincident at the two PMTs were recorded, and 16 output density matrices $\{\mathcal{E}(\rho_{12})\}$ were evaluated by state tomography[18]. Note that we used unnormalized output density matrices because the

state filtering is trace-decreasing process whose output intensity depends on the input state.

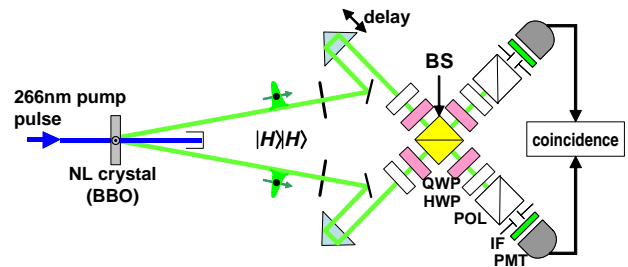


FIG. 1: Experimental setup to characterize the beamsplitter.

We used optical trombones to equalize the two path lengths to within the coherence length of the down-converted photons ($l_c \approx 200 \mu\text{m}$). Two two-photon amplitudes contributing to coincidence detection—*i.e.*, that both photons are reflected (r - r) or that both are transmitted (t - t)—were initially ($\tau = 0$) aligned to overlap both spatially and temporally, giving a HOM dip visibility of 85% as shown in Fig. 2. In this case, the BS is commonly thought to work as a singlet-state filter[12, 13]. To investigate the nonideal filter, we introduced a delay τ in one arm by moving one of the trombone prisms. The larger the τ is, the smaller the overlap of the two amplitudes is and the more the temporal and polarization information of the photon pair is entangled. We will show later that this results in decoherence if we observe only the polarization information.

The process matrices associated with three-delay conditions ($\tau = 0, 100, \text{ and } 350$ fs) were obtained. To make the results clear, we represented them in the non-local operator basis $\{F_{[ij]}\} = \{(E_i \otimes E_j)U_S\}$, where $U_S = 1/2\sum_{i=0}^3\sigma_i \otimes \sigma_i$ is a swap operator. The obtained process matrices χ^F are shown in Fig. 3, where space is saved by showing only the real parts. What is most interesting is that the contribution of $(\chi^F)_{[33][33]}$ element is large and increases with increasing delay τ .

This result is consistent not with the common belief but with what was pointed out in Ref. [9]. Indeed, we found that the results are well reproduced if we assume that $\mathcal{E}(\rho)$ has an operator-sum representation with two Kraus operators \mathcal{P}^- and \mathcal{P}^+ [1]:

$$\mathcal{E}(\rho) = (1-p)\mathcal{P}^-\rho\mathcal{P}^{-\dagger} + p\mathcal{P}^+\rho\mathcal{P}^{+\dagger}, \quad (5)$$

$$\mathcal{P}^\pm = \mathcal{T}U_I \pm \mathcal{R}U_3(\theta_1, \theta_2)U_S, \quad (6)$$

where p ($0 \leq p \leq 1/2$) is a parameter that can be interpreted as the degree of decoherence and where $U_3(\theta_1, \theta_2) = e^{i\theta_1\sigma_3/2}\sigma_3 \otimes e^{-i\theta_2\sigma_3/2}\sigma_3$, which explains the large contribution of the $(\chi^F)_{[33][33]}$ element. The first term of Eq. 5 is an ideal operation for this state-filter and the second term is a noise contribution. Note that Kraus operators are not unique and not necessarily orthogonal[1]. Figure 4 shows the process matrices calculated using the measured value $\mathcal{R}/\mathcal{T} = 0.76$ and appropriate values of the parameters θ_1, θ_2 , and p . As shown

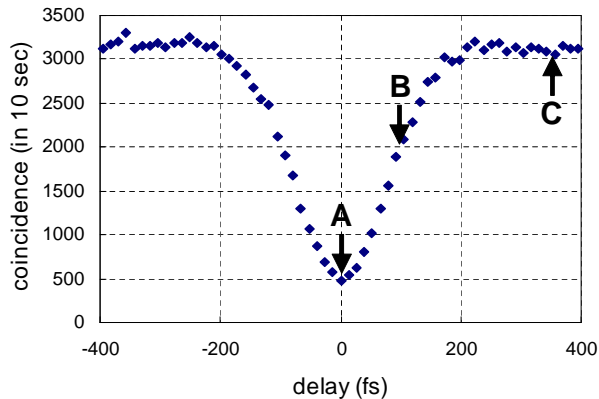


FIG. 2: HOM dip observed in the coincidence record. Arrows indicate the data for (A) $\tau = 0$, (B) $\tau = 100$ fs, and (C) $\tau = 350$ fs delay introduced in one of the two arms.

in Fig. 4, Eqs. 5 and 6 well reproduced the experimental results. It follows that the operator \mathcal{P}^- describing ideal operation deviates from the singlet state because of the factor $U_3(\theta_1, \theta_2)$, which is consistent with Ref. [9].

To understand these results, we need a decoherence model. Let us first reconsider the function of the BS in the polarization space. Let a and b (c and d) denote field operators for two input (output) modes of the BS, and let the polarization of these operators be denoted by subscripts (*e.g.*, by a_H and a_V for the H - and V -polarized field operators). If we use a reference frame in which the positive directions of H - and V -polarized fields of the input and transmitted fields are defined consistently, the equations for the field operators are given by

$$\begin{aligned} c_H &= \sqrt{\mathcal{T}}a_H + ie^{i(\Gamma+\pi)}\sqrt{\mathcal{R}}b_H, \\ d_H &= ie^{-i(\Gamma+\pi)}\sqrt{\mathcal{R}}a_H + \sqrt{\mathcal{T}}b_H, \\ c_V &= \sqrt{\mathcal{T}}a_V + ie^{i\Delta}\sqrt{\mathcal{R}}b_V, \\ d_V &= ie^{-i\Delta}\sqrt{\mathcal{R}}a_V + \sqrt{\mathcal{T}}b_V, \end{aligned} \quad (7)$$

where \mathcal{T} and \mathcal{R} are respectively the transmission and reflection coefficients of the BS. We have assumed that each polarization component of the field acquires a different phase shift $\Gamma + \pi$ and Δ on reflection at the BS. The factor π accounts for the mirror-image effect [19], that is, that the positive direction of the H -polarized field changes on reflection at near normal incidence. This may change the helicity of the polarization of the reflected fields. Although the incidence angle in our interferometer was 45° , we did observe helicity reversal. For example, when the incident light was diagonally polarized, we found that the transmitted light was diagonally polarized and the reflected light was almost anti-diagonally polarized. From Eqs. 7, if we consider the output fields that can contribute to coincidence measurement, we conclude that the BS projects the input state onto \mathcal{P}^- with $\theta_1 = \theta_2 = \Delta - \Gamma$. Note that the projector \mathcal{P}^- is the coherent sum of the identity operator U_I associated with

transmission and the operator $U_3(\theta_1, \theta_2)U_S$ associated with reflection, where $U_3(\theta_1, \theta_2)$ accounts for the helicity reversal and the polarization dependent phase shift of reflected fields.

Although the above description may suffice when $\tau = 0$, the temporal (T) space of the two-photon state should be taken into account when $\tau \neq 0$. Concerning the temporal state space, it would be reasonable to assume that the BS leaves the state untouched on transmission and swaps the state on reflection. We thus assume that the function of the BS is described by the following operator entangled with respect to the polarization and temporal state spaces:

$$\mathcal{P}^{PT} = \mathcal{T}U_I^P \otimes U_I^T - \mathcal{R}U_3^P(\theta_1, \theta_2)U_S^P \otimes U_S^T, \quad (8)$$

where the superscripts indicate the space on which each operator acts. We further assume that input state is unentangled, *i.e.*, that it is a product state of polarization state ρ^P and temporal state σ^T . Then, by partially tracing over the temporal degree of freedom, we obtain the following output polarization state $\mathcal{E}^P(\rho^P)$ consistent with Eqs. 5 and 6:

$$\begin{aligned} \mathcal{E}^P(\rho^P) &= \text{Tr}_T \mathcal{P}^{PT} (\rho^P \otimes \sigma^T) (\mathcal{P}^{PT})^\dagger \\ &= (1-p)\mathcal{P}^P \rho^P \mathcal{P}^{P\dagger} + p\mathcal{Q}^P \rho^P \mathcal{Q}^{P\dagger}, \end{aligned} \quad (9)$$

where the parameter p ($0 \leq p \leq 1/2$) depends on the overlap of the two-photon amplitudes contributing to coincidence detection (r - r or t - t) and thus on the delay τ . Ideally, p is unity if $\tau = 0$ and is a decreasing function of τ . Figure 4 shows that this model largely explains the experimental results, except that θ_1 is not actually equal to θ_2 as in the model. The reason is uncertain, but this inequality may be due to polarization-dependent \mathcal{R}/\mathcal{T} ignored in the model.

We conclude that the function of the ideal BS is described by \mathcal{P}^- , which depends on the phase shifts Γ and Δ as well as the coefficients \mathcal{R} and \mathcal{T} . These parameters obviously depend on the detailed design of the BS. It might be possible to achieve $\mathcal{R}/\mathcal{T} = 1$ and $\Gamma = \Delta = 0$ for light incident at 45° , at least for photons with a particular wavelength by designing the BS appropriately. In this idealized case, \mathcal{P}^- agrees with one of the four Bell states: a triplet state. This shows that the common belief that a BS with post-selection works as a singlet-state filter is erroneous. This error is a result of overlooking the helicity reversal occurring on photon reflection.

In summary, we used QPT to investigate the non-ideal two-qubit quantum-state filter and identify its function. The results were satisfactorily explained by a simple model with several reasonable assumptions. We pointed out an error in a common belief about the function of a BS with post-selection.

We thank S. Ishizaka and A. Tomita for their helpful discussions. This work was supported by the CREST program of the Japan Science and Technology Agency.

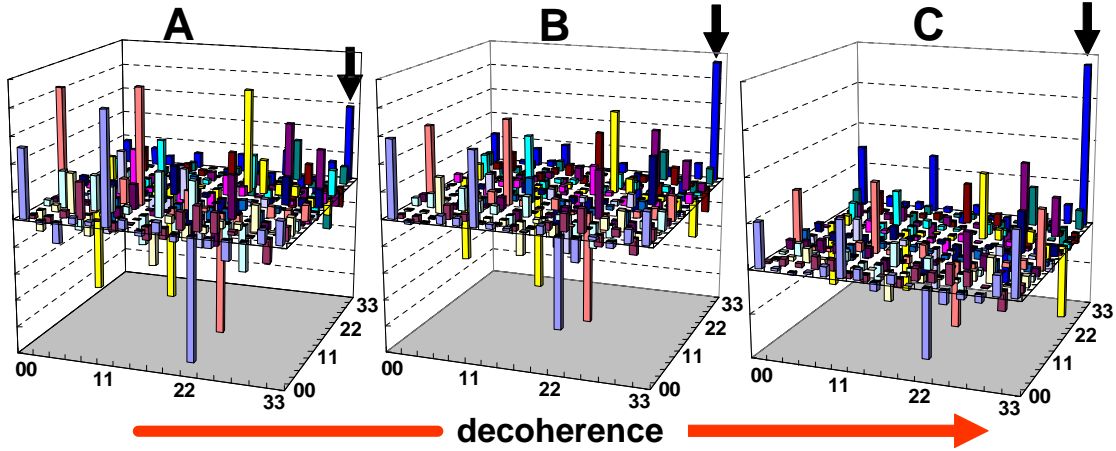


FIG. 3: The process matrices of the beamsplitter obtained for (A) $\tau = 0$, (B) $\tau = 100$ fs, and (C) $\tau = 350$ fs. Only the real parts of the matrices are shown in arbitrary units. Vertical arrows indicate the diagonal elements $(\chi^F)_{[33][33]}$.

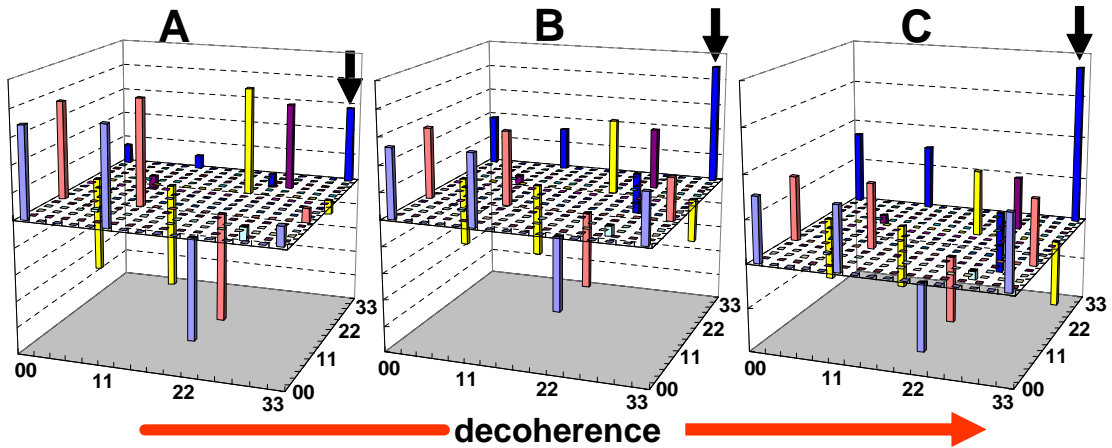


FIG. 4: Calculated process matrices corresponding to Fig. 3 (see text). The following parameters were used: (A) $p = 0.14$, (B) $p = 0.325$, (C) $p = 0.5$ and the common parameters $\mathcal{R}/\mathcal{T} = 0.76$, $\theta_1 \approx 0.41\pi$, and $\theta_2 \approx 0.076\pi$.

-
- [1] I. L. Chuang and M. A. Nielsen, *Quantum Information and Quantum Computation* (Cambridge University Press, Cambridge, 2000).
- [2] I. L. Chuang and M. A. Nielsen, *J. Mod. Opt.* **44**, 2455 (1997).
- [3] J. F. Poyatos *et al.*, *Phys. Rev. Lett.* **78**, 390 (1997).
- [4] G. M. D'Ariano and P. Lo Presti, *Phys. Rev. Lett.* **86**, 4195 (2001); *Phys. Rev. Lett.* **91**, 047902 (2003).
- [5] Y. Nambu *et al.*, *Proc. SPIE Int. Soc. Opt. Eng.* **4917**, 13 (2002).
- [6] J. B. Altepeter *et al.*, *Phys. Rev. Lett.* **90**, 193601 (2003).
- [7] F. De Martini *et al.*, *Phys. Rev. A* **67**, 62307 (2003).
- [8] A. M. Childs *et al.* *Phys. Rev. A* **64**, 12314 (2001).
- [9] M. W. Mitchell *et al.*, *Phys. Rev. Lett.* **91**, 120402 (2003).
- [10] J. L. O'Brien *et al.*, *quant-ph/0402166*.
- [11] C. K. Hong *et al.*, *Phys. Rev. Lett.* **59**, 2044 (1987).
- [12] K. Mattle *et al.*, *Phys. Rev. Lett.* **76**, 4656 (1996).
- [13] S. L. Braunstein and A. Mann, *Phys. Rev. A* **51**, R1727 (1995).
- [14] K. Kraus, *State, Effects, and Operations*, Lecture Notes in Physics Vol. 190 (Springer, Berlin, 1983).
- [15] P. Rungta *et al.*, *quant-ph/0001075*; P. Rungta *et al.*, *quant-ph/0102040*.
- [16] G. M. D'Ariano *et al.*, *Phys. Lett. A* **272**, 32 (2000).
- [17] J. I. Cirac *et al.*, *Phys. Rev. Lett.* **86**, 544 (2001); W. Dür *et al.*, *Phys. Rev. A* **64**, 12317 (2001).
- [18] Y. Nambu *et al.*, *Phys. Rev. A* **66**, 33816 (2002).
- [19] J. M. Bennett, in *Handbook of Optics*, edited by M. Bass (McGraw-Hill, New York, 1995), Chap. 5.